The Ability of Regional Climate Models to Simulate Weather Conditions on Nordenskiöldbreen, Svalbard

Regionala klimatmodellers förmåga att simulera väderförhållanden på Nordenskiöldbreen, Svalbard

Malin Andersson
Erica Erikson

UPPSALA
UNIVERSITET

DEPARTMENT OF
EARTH SCIENCES

INSTITUTIONEN FÖR
GEOVETENSKAPER

The Ability of Regional Climate Models to Simulate Weather Conditions on Nordenskiöldbreen, Svalbard

Regionala klimatmodellers förmåga att simulera väderförhållanden på Nordenskiöldbreen, Svalbard

Malin Andersson

Erica Erikson

Abstract

The Ability of Regional Climate Models to Simulate Weather Conditions on Nordenskiöldbreen, Svalbard

Malin Andersson, Erica Erikson

In this project, we analyse the ability of two regional climate models to simulate meteorological conditions on Nordenskiöldbreen, a glacier in Svalbard. To do so, regional climate model output is compared with in situ measurements from an automatic weather station. Detailed information about the weather conditions on Nordenskiöldbreen is important for simulating the glacial mass balance in a changing climate. The parameters analysed were the following: temperature, air pressure, relative humidity, precipitation, cloud cover, wind speed and wind direction. The weather station did not measure all parameters, cloud cover was instead estimated through the incoming longwave radiation and temperature, while precipitation was calculated from snow depth. The results show that the models represent certain parameters better than others. Temperature, air pressure and wind speed and direction are found to be simulated with high precision. Poorest agreement is found for precipitation, which appears to be both difficult to simulate and observe. Relative humidity and cloud cover show average agreement with the station.

The conclusion of the project is that the estimation of some of the parameters is satisfactory, while others are lacking. None of the models can be determined to have performed significantly better than the other.

Sammanfattning

Regionala klimatmodellers förmåga att simulera väderförhållanden på Nordenskiöldbreen, Svalbard

Malin Andersson, Erica Erikson

I det här projektet analyserades två regionala klimatmodellers förmåga att simulera meteorologiska förhållanden på Nordenskiöldbreen, en glaciär på Svalbard. Detta gjordes genom jämförelser av data från regionala klimatmodeller mot lokala mätningar från en automatisk väderstation. Detaljerad information om väderförhållandena på Nordenskiöldbreen är viktigt för att kunna simulera glaciärens massbalans i ett föränderligt klimat. Parametrarna som jämfördes var temperatur, lufttryck, relativ luftfuktighet, nederbörd, molntäcke samt vindhastighet och vindriktning. Stationen mätte inte alla parametrar, molntäcket uppskattades istället genom inkommande långvågig strålning och temperatur, medan nederbörd beräknades via snödjup. Resultatet visar att modellerna representerar vissa parametrar bättre än andra. Temperatur, lufttryck, vindhastighet och vindriktning simuleras med hög precision. Parametern med lägst samband är nederbörd, som verkar vara svår både att simulera och observera. Relativ luftfuktighet och molntäcke har ett medelmåttigt samband till stationen.

Slutsatsen av projektet är att modellernas uppskattning av några parametrar är tillräckligt bra, medan andra är bristfälliga. Ingen av modellerna kan bedömas ha presterat signifikant bättre än den andra.

Table of Contents

1.   Introduction

Changes in the global climate conditions have led to an increase in temperature, with the trend of rising temperature being stronger in the Arctic compared to lower latitudes (IPCC 2013). Contributors to this are positive feedback processes, the most pronounced ones relating to changes in sea ice cover (Screen & Simmonds 2010). Due to the summer sea ice extent decreasing over the past decades and the seasonal period of melting extending, large oceanic surfaces are exposed. This leads to a lowering of the albedo and allows more solar radiation to be absorbed in the ocean surface (Screen & Simmonds 2010). The stored energy is released to the atmosphere during winter, raising the temperature further, a process referred to as Arctic amplification (Serreze et al. 2009; Bintanja & Van der Linden 2013).

   Since glaciers are such strong indicators of the global climate, studying them and estimating the mass balance can give an extensive quantity of information about variations in the climate. Depending on the meteorological trend, the glacier either accumulates mass or undergoes ablation, and the relationship between these constitutes the glacial mass balance (Tarbuck et al. 2014; Cogley et al. 2011). Mass balance estimations are commonly made using the surface energy budget of a glacier. The energy balance is constructed from the total amount of energy fluxes at the glacial surface, for which the meteorological conditions need to be known (Ebrahimi & Marshall 2016). Information about the conditions can be obtained either through in situ weather stations or using regional climate models (RCMs) (Benn & Evans 1998).

   The meteorological data used in the project was gathered from the Nordenskiöldbreen Glacier (Figure 1), located on the Arctic island Spitsbergen, a part of the Norwegian archipelago Svalbard (Hagen et al. 2003). Svalbard is covered to 60% with glacial ice, an area of 36 600 km^2 and a volume of 7000 km^3 (Hagen et al. 2003). The local climate on Svalbard is relatively mild due to its placement at the end of the Atlantic current, which brings warm water to the northern latitudes (Van Pelt 2014). Nordenskiöldbreen is an outlet glacier of the ice plateau Lomonosovfonna and extends as a valley glacier between De Geerfjellet and Terrierfjellet (Walczowski & Piechura 2006). The average flow speed along the flow line varies between 40 and 55 m/year, with measured peaks of 60 m/year (Den Ouden et al. 2010; Van Pelt et al 2018). Nordenskiöldbreen is a tidewater type glacier, which means that it terminates in the sea, where calving occurs on the glacial front (Tarbuck et al. 2014).

   The remote location of the archipelago in combination with the climate conditions lead to difficulties maintaining an automatic weather station (AWS) for a long continuous period. Disruptions in the monitoring can be caused by rime, i.e. ice accretion on the sensors, or by short circuiting from meltwater leaking in to the equipment or logger box. This leads to periods with inaccurate or missing data. RCMs provide continuous data and cover a larger area than the AWS, which only measures the conditions for a specific point. The RCMs do however need to be

validated against an AWS in order to determine whether or not they provide correct meteorological data.

The purpose of this project is to compare and validate the ability of two regional climate models to simulate meteorological conditions on Nordenskiöldbreen glacier. Thereby determining if it is possible to use simulated conditions for mass balance modelling (Van Pelt et al. 2012; Van Pelt & Kohler 2015). The project aims to answer the questions of how well HIRLAM and RACMO can describe weather conditions on a High Arctic glacier and which one, if any, of the two models can give the most accurate result. This will be done by comparing RCM output of temperature, humidity, air pressure, relative humidity, cloud cover and precipitation, as well as wind speed and direction, with observations from Nordenskiöldbreen on Svalbard.
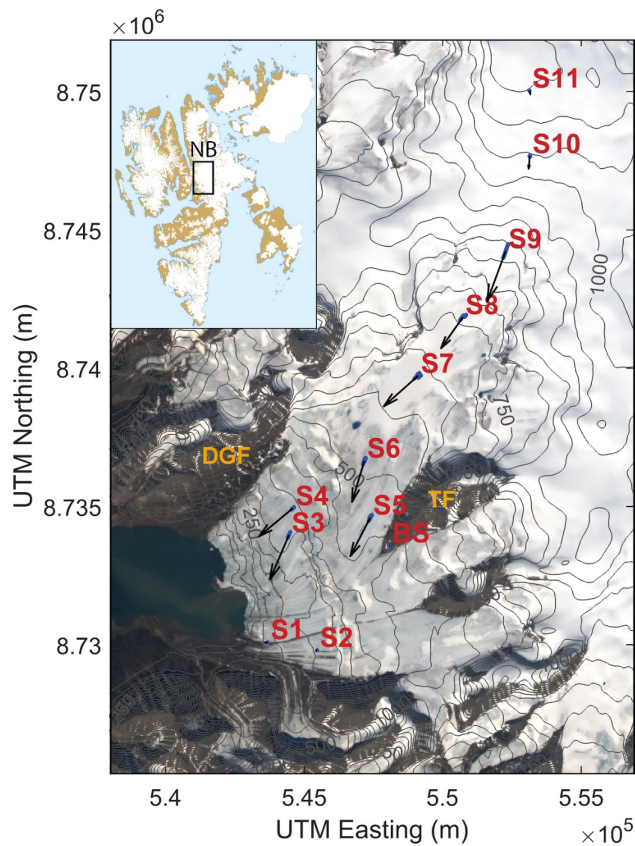

Figure 1. Map of Nordenskiöldbreen and surrounding area with flow direction indicated by the arrows. The background image is based on NASA Landsat imagery from 2002 and the height contours are from a digital elevation model from the Norwegian Polar Institute (NPI).

2. Theory and methods

The parameters analysed in this project have an impact on glacial mass balance and affect the growth and melt of a High Arctic glacier. Temperature is a critical factor which determines whether a glacier will accumulate mass or not, which in turn is affected by the altitude of the site. For every kilometre of elevation increase, the temperature drops by an estimated 6-7 °C (Oerlemans 2010). Melting is amplified by parameters such as relative humidity and wind strength. Even though the temperature remains unchanged, days with strong wind and high relative humidity

generate higher melt rates than still days with low relative humidity (Benn & Evans 1998). High wind speeds cause a turbulent heat exchange and the increase in humidity generate a latent heat flux, triggered when the condensated water at the glacier surface release excess heat and bring about additional melting (Benn & Evans 1998). Cloud cover changes the supply of incoming longwave radiation, which affects the temperature and thereby the melting (Kuipers Munneke et al. 2011). Precipitation is another important factor influencing the mass balance, due to its impact on snow accumulation. Wind direction over a glacier is dominated by the katabatic flow, occurring when the glacier cools the near surface air, increasing the density and creating a downslope flow (Oerlemans 2010; Vihma et al. 2011). An anabatic flow is common in the opposing direction of the katabatic wind. The process of gaining momentum is slow, and with limited stretches of glacial surface, the wind speeds remain stable at a low velocity (Oerlemans 2010).

2.1. Automatic weather station

The local meteorological measurements are gathered using an automatic weather station (Figure 2) installed on Nordenskiöldbreen, which records information with an hourly interval. The station is located at 531 meters above sea level, in between the two mountains, De Geerfjellet and Terrierfjellet (Van Pelt 2014). Equipped with devices for documenting snow depth, temperature, relative humidity, air pressure, incoming longwave radiation, wind speed and wind direction, the station provides a great deal of information regarding the local climate conditions. However, the remote location of the AWS limits the maintenance visits to once a year, meaning equipment cannot be repaired or replaced in case of malfunctioning in between visits. The RCMs can be a useful alternative, since they cover a larger area and deliver continuous measurements.
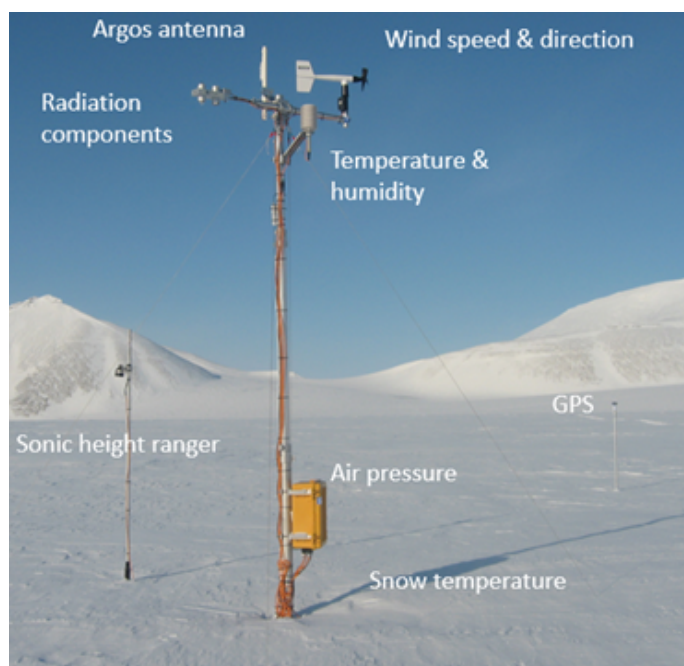

Figure 2. The automatic weather station on Nordenskiöldbreen. Photo taken by Carleen Tijm-Reijmer.

2.2. Climate modelling

Regional climate models are used to simulate the meteorological conditions and have a higher spatial resolution than global climate models [http://ukclimateprojections.metoffice.gov.uk].

Two regional climate models are used in this project, the High Resolution Limited Area Model (HIRLAM; Reistad et al. 2011) and the Regional Atmospheric Climate Model 2.3 (RACMO; Noël et al. 2016). HIRLAM has a grid size of 11×11 km, while RACMOs grid size is 3.5×3.5 km (Van Pelt et al. 2016). The models cover the whole of Svalbard, but only data from the grid cells closest to the weather station was used. Figure 3 shows these cells as well as the location of the AWS. Both models use three hourly time fields. The altitudes of the models differs quite a lot. The HIRLAM grid cell is located at 477 meters above sea level, while the RACMO grid cell is at 554 m.a.s.l.
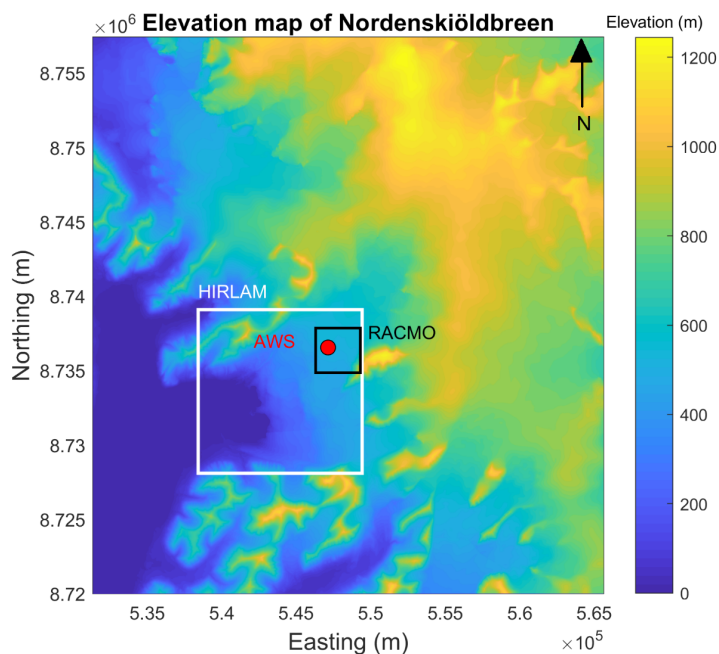

Figure 3. Elevation map of Nordenskiöldbreen with the AWS and the closest cells of HIRLAM and RACMO marked.

2.3. Methods

Data from the models and the AWS from the years 2009-2016 was used in this project, as well as a digital elevation map (DEM) collected by the Norwegian Polar Institute [http://geodata.npolar.no]. This section describes the methods used to compare the three datasets.

2.3.1. Data processing and analysis

A large part of the processing of the AWS data had been made prior to the project, such as removal of outliers due to insufficient data logging because of riming and short circuiting. During the project additional outliers were removed.

The parameters available for both of the models and the weather station were compared; temperature (section 3.1.), air pressure (section 3.2.) and relative humidity (section 3.3.). Wind speed and wind direction data were also analysed (section 3.6.) but only for the AWS and RACMO, since wind data for HIRLAM was not included in the data set. The parameters precipitation and cloud cover were not measured directly by the weather station and therefore had to be estimated. Precipitation was estimated based on snow depth (section 3.4.). Cloud cover was estimated using incoming longwave radiation and temperature data (section 3.5.).

2.3.2. Calculating precipitation

By multiplying the snow depth measured by the weather station's sonic ranger with the density of snow, precipitation could be approximated. Snow density varies, but based on snow pit measurements on Nordenskiöldbreen, a fixed value of 0.4 kg/m^3 was used for the calculations (Van Pelt et al. 2012). Because of the uncertainty of this estimation, and since the snow depth can change a lot depending on the wind, the calculations were made on the daily means of the snow depth. First, the MATLAB function `diff` was used to calculate the difference in snow depth of each day. Of the resulting values, negative ones were set to 0, since that means snow has melted more than it accumulated or that it has been blown away. The positive values were multiplied by the density of snow. Two synchronized timetables containing the precipitation values of the models and the calculated snow accumulation from the station were made, one with daily values and one with monthly.

2.3.3. Estimating cloud cover

Incoming longwave radiation increases with both cloudiness and air temperature, which means that cloud cover can be estimated by using the measured temperature and incoming longwave radiation (Kuipers Munneke et al. 2011). Figure 4 shows the relationship between incoming longwave radiation and temperature.
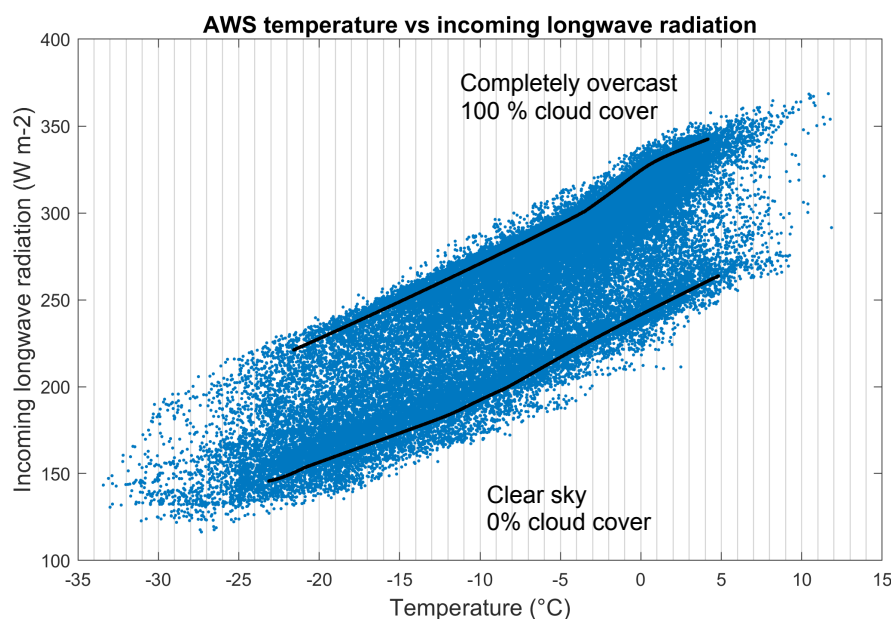

Figure 4. Temperature vs incoming longwave radiation data from the AWS, the black lines show the relationship with cloud coverage.

The data was divided into bins with a temperature span of 1 degree, using the discretize function. The top 10% of the incoming longwave radiation in each bin were assigned to represent 100% cloud cover, and the bottom 10% were assigned a value of 0% cloud cover. Bins with too small data amount (>20 elements) were assigned NaN values. In time periods where temperature or radiation data were missing, no estimation of cloud cover was performed, instead the corresponding values were set to NaN. The values of each bin used were thereafter interpolated linearly to estimate cloud cover percentage. The resulting values were then combined with the NaN values and used as the cloud cover parameter for the AWS.

2.3.4.   Wind speed and direction

Using the wind data from the station and RACMO, two wind roses and two histograms were created, one of each for the data sets. The wind roses were made with the function `WindRose` made by Daniel Pereira [https://se.mathworks.com/matlabcentral/fileexchange/47248-wind-rose] and they show the wind speeds and directions. The function `hist` was used to draw histograms showing the number of occurrences of wind directions in the area.

2.3.5.   Timetables and synchronizations

The weather station and the two RCMs gathered data at different time intervals, the data sets therefore had to be converted to the same time resolution in order to enable comparison. MATLAB was used to create common time-vectors, called timetables, for the data sets. One timetable was made for the station and one for each of the models. They were then synchronized into joint timetables with mean values in time spans of 3 hours, days and months. Precipitation however, was only synchronized in daily and monthly time spans, since sums had to be used instead of the mean and 3 hourly precipitation values are too small to distinguish from sensor noise.

2.3.6.   Statistical tools

Periods without data captured by the AWS can negatively affect data analysis by, for example, shifting a yearly temperature mean towards lower values if the station was malfunctioning during summer. To be consistent when comparing averaged data, the periods of missing data were removed from both the AWS and RCM time-series before creating scatterplots. This was done by removing the rows where the weather station was malfunctioning from the common timetables for each parameter. The scatterplots were made with the function `scatter` and compare the models against the station and against each other for each of the parameters, except wind.

Correlation coefficients were calculated for the 3 hourly values of the parameters, except for precipitation, where daily values were used. This was done using the function `corrcoef`, which also gave the significance of the correlation (p-value). The bias was determined by subtracting the means of each parameter as described by the following pseudo code:

```
% Bias temperature:
bias_temperature_hir_aws = mean(HIRLAM)- mean(AWS);
bias_temperature_hir_rac = mean(HIRLAM)- mean(RAC);
bias_temperature_rac_aws = mean(RAC)-mean(AWS);
```
The function `rms` was used to measure the root mean square error (RMS). This was done by first subtracting the parameters of one data source from another, and then applying the function.

3. Results and discussion

In this section, we present and discuss the comparison of regional climate model output and observed weather conditions on Nordenskiöldbreen. The mean, the correlation coefficients, the RMS and the bias are calculated for 3-hour resolution, for all parameters except precipitation, which uses the daily sum. A list of the functions used to calculate the results can be found in the appendix.

The correlation coefficients showed positive correlations for all parameters (Table 1). Additionally, all the p-values were below 0.05, which means that all the correlation coefficients are significant are significant at the 95-% confidence limit..Table 2 displays the mean of each parameter for each data source. Bias and RMS are shown in Table 3 and Table 4 respectively.

Table 1. The correlation coefficients (R) of the parameters temperature (T), relative humidity (RH), air pressure (AP) precipitation (P), cloud cover (CC). The first two rows show the correlation coefficients between the weather station and the models, while the third rows shows the relation between RACMO and HIRLAM.

Corrcoef (R)	T	RH	AP	P	CC
RACMO-AWS	0.92	0.38	0.98	0.27	0.53
HIRLAM-AWS	0.94	0.47	0.98	0.089	0.53
RACMO-HIRLAM	0.91	0.39	1.00	0.39	0.63

Table 2 Shows the mean of the parameters temperature (T), relative humidity (RH), air pressure (AP) precipitation (P), cloud cover (CC) and wind speed (WS).

Mean	T (°C)	RH (%)	AP (Pa)	P (mm)	C (%)	WS (m/s)
RACMO	-9.13	85.47	94320	2.23	57.57	3.39
HIRLAM	-8.64	83.02	95075	2.89	65.69	-
AWS	-8.04	84.17	94340	2.00	56.96	4.57

Table 3. Bias for the parameters temperature (T), relative humidity (RH), air pressure (AP) precipitation (P), cloud cover (CC) and wind speed (WS). The first two rows show the bias between the models and the AWS respectively, the last row shows the bias between the models.

Bias	T (°C)	RH (%)	AP (Pa)	P (mm)	CC (%)	WS (m/s)
RACMO-AWS	-1.087	1.30	-20.18	0.23	0.61	-1.18
HIRLAM-AWS	-0.60	-1.14	735.15	0.86	8.73	-
HIRLAM-RACMO	0.49	-2.45	755.30	0.63	8.12	-

Table 4. Root mean square error for the parameters temperature (T), relative humidity (RH), air pressure (AP) precipitation (P), cloud cover (CC) and wind speed (WS). The first row shows the RMS between RACMO and the AWS, the second HIRLAM and the AWS, and the third displays the RMS between the two models.

RMS	T (°C)	RH (%)	AP (Pa)	P (mm)	CC (%)	WS (m/s)
RACMO-AWS	3.49	12.66	209.05	7.32	36.95	2.76
HIRLAM-AWS	3.46	10.88	764.99	7.45	38.87	-
HIRLAM-RACMO	4.02	12.09	762.28	6.38	36.39	-

3.1. Temperature

The plots of temperature over time (Figure 5) in monthly time resolution show that the simulated values are well in agreement with the measurements from the weather station. In the daily and 3 hourly resolutions the RCMs can be seen deviating from the AWS for shorter periods, before aligning again.

Scatterplots (Figure 6) and the correlation coefficients indicate high correlations between the RCMs and the AWS, with slightly better correlation between HIRLAM and the station (R=0.94 vs R=0.92 for RACMO). The two models simulate values that are more similar to the weather station's at temperatures closer to 0°C, for lower temperatures, the scatter spread is wider. The models agree better with the AWS than with each other. The RMS between the two models and the station are both about 3.5°C, while the RMS between the RCMs is a bit higher at 4.0°C. The mean shows that the station measured slightly higher temperatures than the models during the time period. All the comparisons return a rather low bias.
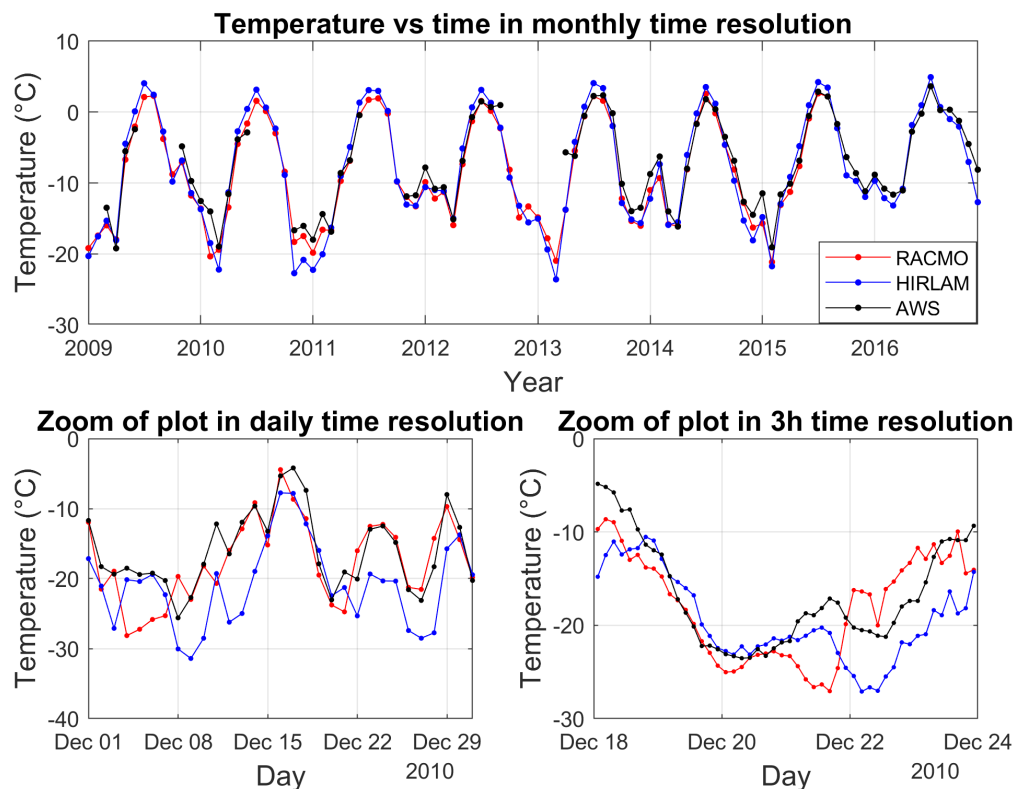

Figure 5. Plots of temperature vs time in monthly (top), daily (bottom left) and 3 hour (bottom right) time resolutions. The coloured lines represent the AWS (black), RACMO (red) and HIRLAM (blue).
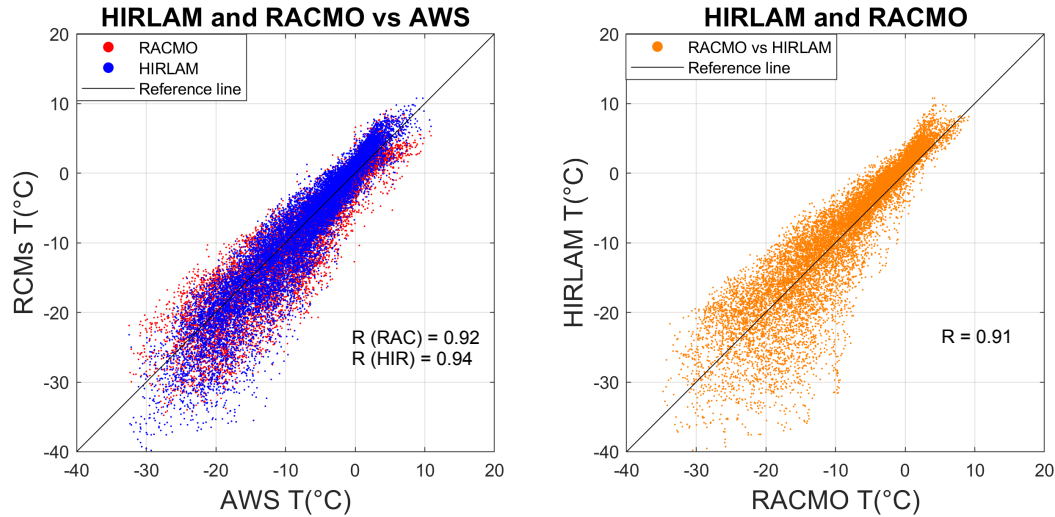
8

Figure 6. Scatterplot of RCMs vs AWS (left) and scatterplot of HIRLAM vs RACMO (right).

The models represent seasonal changes well, although HIRLAM appears to be overestimating temperatures in summer and presenting lower values for the winter periods. Since the correlation coefficients between the models and the AWS are slightly higher than the correlation coefficient between the models themselves, it means that both models simulate temperature slightly closer to the measured site temperature, than to each other. The reason for this might be the difference in elevation of almost 80 meters between the RCMs, with the station located in between them, since the temperature is lower at a higher altitude. This can also be seen in the bias, where the value of RACMO and the AWS is negative, since the station is located at a lower elevation. Similarly, the bias between the two models is positive, meaning that RACMO shows a lower mean temperature than HIRLAM does, probably due to its elevation. However, the bias between HIRLAM and the station is also negative, although slightly less, despite the station being located at a higher elevation. The fact that the RMS between the models is higher than with the AWS is to be expected with the large difference in elevation between the RCMs.

Overall both models simulate temperature well, but their accuracy decreases in colder weather. HIRLAM might be slightly better at the task, when considering it has a somewhat higher correlation coefficient as well as lower bias and RMS.

3.2. Air pressure

The RCMs model the air pressure in close agreement to measurements taken in situ by the AWS (Figure 7). Regardless of resolution, the models and the weather station follow the same trends. RACMO returns values close to the AWS, while HIRLAM has a continuous overestimation. The high correlations are further seen in the scatterplots where RACMO plotted against the AWS consistently follows the reference line (Figure 8). The correlation coefficients are all close to 1. HIRLAM's overestimation of air pressure can be seen in the scatterplots as well as in the bias between HIRLAM and the station, 7.35 hPa. The bias between RACMO and the AWS is lower, -0.20 hPa. Similarly, the RMS is lowest for RACMO with the AWS (2.1 hPa) than for HIRLAM with the AWS (7.65 hPa).The means of the different data

sources are very similar, with HIRLAM showing the largest mean air pressure, about 7.00 hPa higher than what the station and RACMO presents.
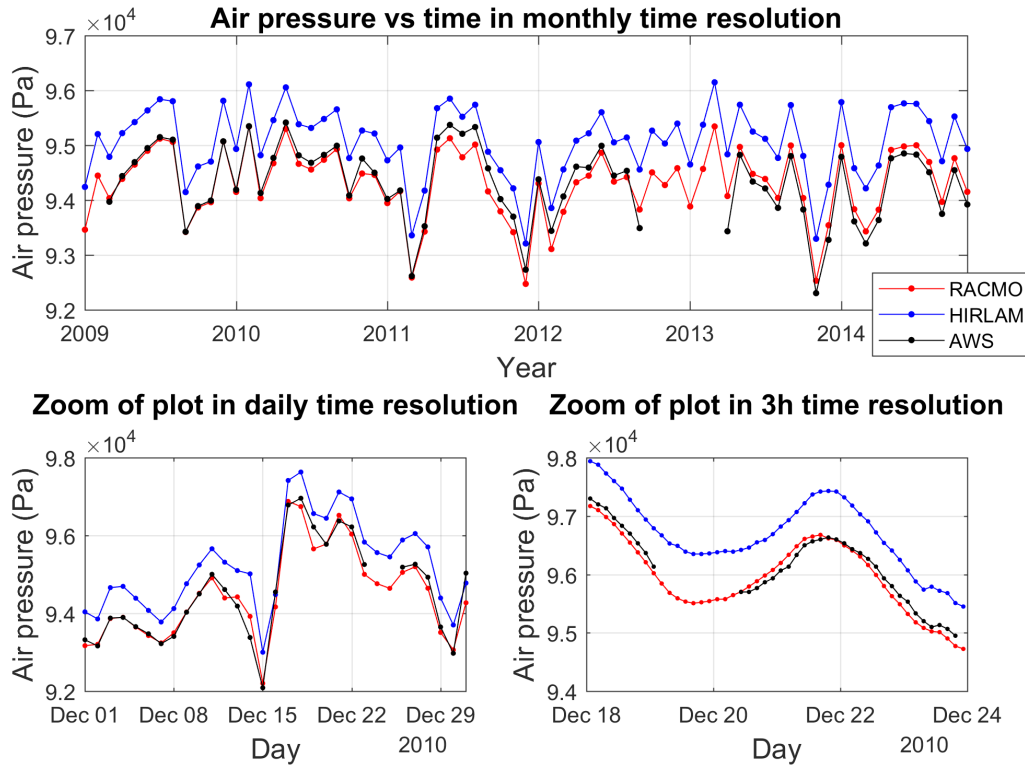

Figure 7. Plots of air pressure vs time in monthly (top), daily (bottom left) and 3 hour (bottom right) time resolutions.
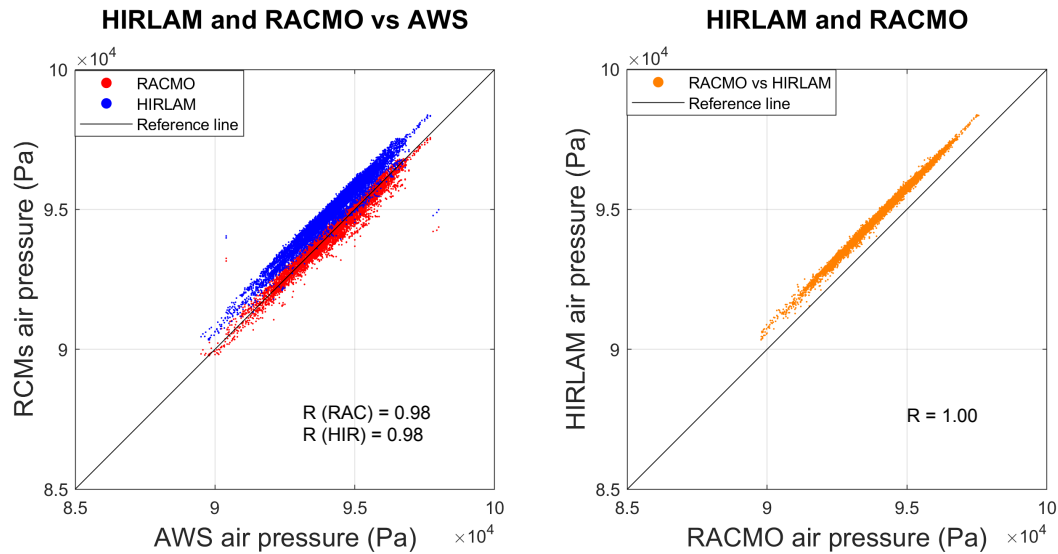

Figure 8. Scatterplot of RCMs vs AWS (left) and scatterplot of HIRLAM vs RACMO (right).

The air pressure is well simulated. As seen in the time-series, both models fit the curve to a very satisfying degree. HIRLAM overestimates the pressure, but this is expected since the pressure decreases with height and HIRLAM is located at the lowest altitude of the data sources. The scatterplots show the overestimation, as does the RMS together with the bias, giving a general overestimation of about 7.35 hPa. The correlation coefficients of air pressure are distinctly higher than all the other parameters', and therefore indicating that the models give accurate values. The correlation coefficient between the two models is a little higher than the ones against

the AWS, which could be a result of temporary malfunctioning pressure sensors. The sensors are dependent on air ventilation and can be affected by riming, which may disturb their measurements slightly.

Both of the models represent the air pressure accurately and they have similar correlation coefficients, but RACMO shows both lower bias, lower RMS and a mean that is closer to the value of the station. Therefore, it might represent air pressure better than HIRLAM does.

3.3.   Relative humidity

The relative humidity plot (Figure 9) in monthly time resolution illustrates how the RCMs for certain periods follow the same trends as the AWS, although with differences in percentage humidity measured. In daily and 3 hourly resolution, it further shows the disagreement between the three sources of data and how the RCMs do not capture minor variations in relative humidity very well. Even though there are variations in relative humidity measured in monthly resolution, both the RCMs and the AWS are in agreement regarding the humidity staying between 70% and 95%. The scatterplots (Figure 10) show a wide spread from the reference line. The correlation coefficients (Table 1) are rather low, but they still show a positive correlation. The highest correlation is between HIRLAM and the AWS, 0.47, and the lowest between RACMO and the AWS, 0.38. The correlation between the models is 0.39 and shows that they are in weak agreement. All the RMS values are rather high, but the value between HIRLAM and the AWS is still the lowest with 11%. All the data sources give a mean of over 80%, with RACMO showing the highest at 85% and HIRLAM the lowest with 83%.
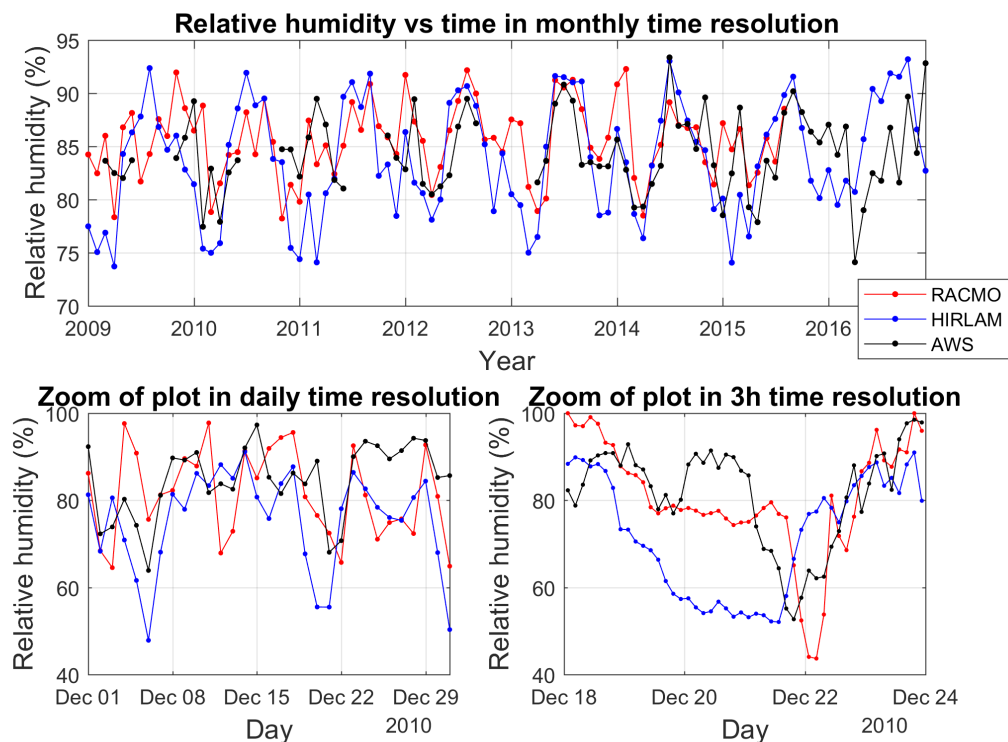

Figure 9. Plots of relative humidity vs time in monthly (top), daily (bottom left) and 3 hour (bottom right) time resolutions.
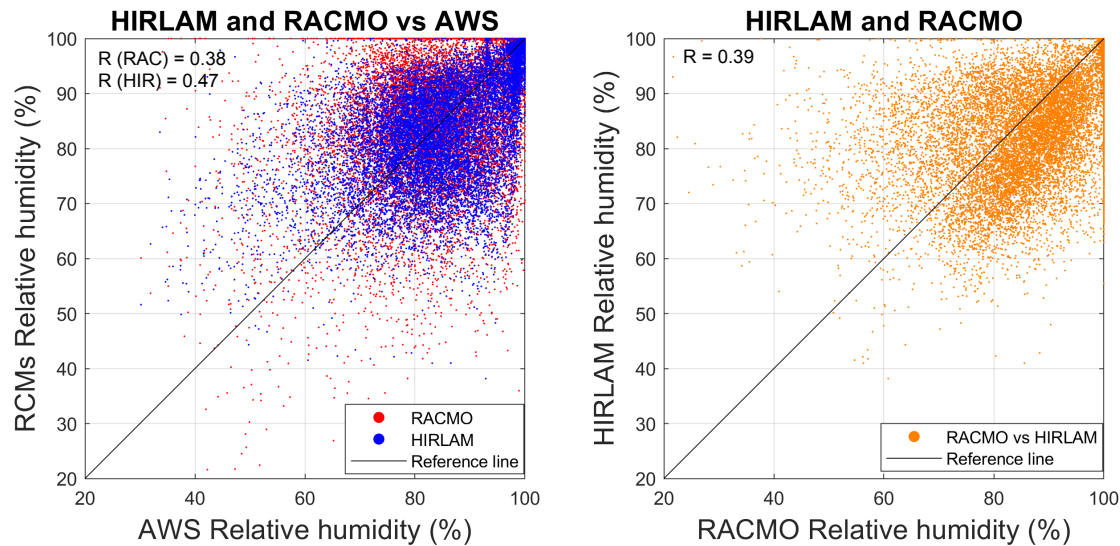
Figure 10. Scatterplot of RCMs vs AWS (left) and scatterplot of HIRLAM vs RACMO (right).

As seen in both the time- and the scatterplots, the models are not as good at predicting the relative humidity as they are at predicting air pressure. The low bias implies that neither one of the models is consistently over- or underestimating the relative humidity. Since the mean does not differ much between the data sources, it suggests that overall the models and the station show similar values.

Relative humidity might be harder to simulate for the models than other parameters, but the results can also be a consequence of the differences in both height and cell size of the data sources. Since HIRLAM covers a larger area than the weather station, it can include local specific humidity variations that does not affect the AWS. Considering that RACMO has a smaller grid cell and a midpoint closer to the AWS, it ought to capture the relative humidity better. Since this is not the case, RACMO has a lower correlation coefficient with the AWS than HIRLAM does, local variations might not be the main cause of the difference between the RCMs and the AWS. A contributor to the low correlation could be how parameters such as air pressure and air temperature directly affect the relative humidity. Failure to capture the full variations in temperature over the glacier will therefore lead to secondary errors in the relative humidity. For this parameter, none of the models performed satisfactory, but HIRLAM was slightly better than RACMO.

3.4. Precipitation

With precipitation plotted over time, there are some slight trends that can be seen in both models and in the data from the weather station. Most of the time, the models simulate higher amounts of precipitation than what is measured in situ (Figure 11). There is rarely any overlap of the actual values provided from the RCM and the AWS. The scatterplots (Figure 12) show low positive correlations between the two RCMs and the AWS. Between RACMO and HIRLAM, the correlation is higher. The correlation coefficient for precipitation when comparing RACMO to the AWS is 0.27, a low positive correlation. HIRLAM measured against the AWS returned a coefficient of 0.085, which is extremely low. The correlation coefficient between the two models is 0.39, indicating a closer similarity between the two models than with the AWS. The

mean values are rather similar, around 2 mm/day, with HIRLAM having the highest mean: 2.89 mm/day. The highest bias and the highest RMS is between HIRLAM and the AWS, 0.89 mm and 7.44 mm respectively.
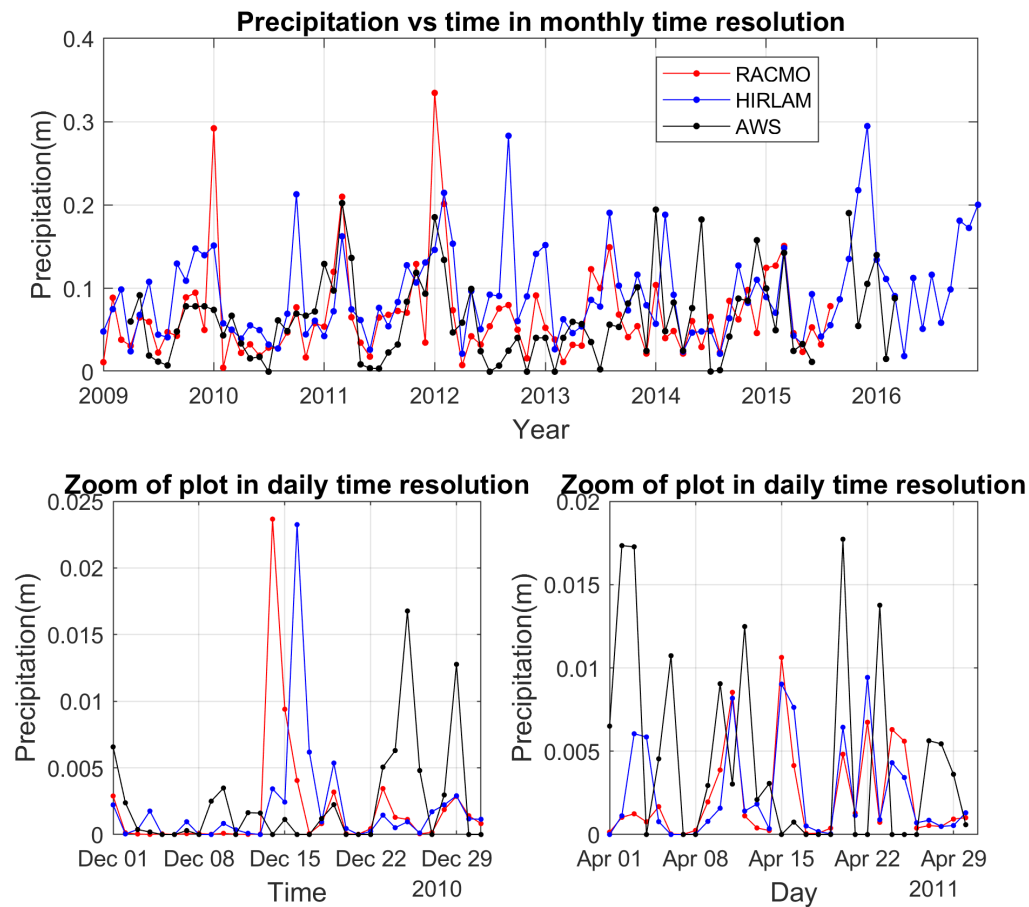

Figure 11. Plots of precipitation vs time in monthly (top) and daily (bottom) time resolutions.
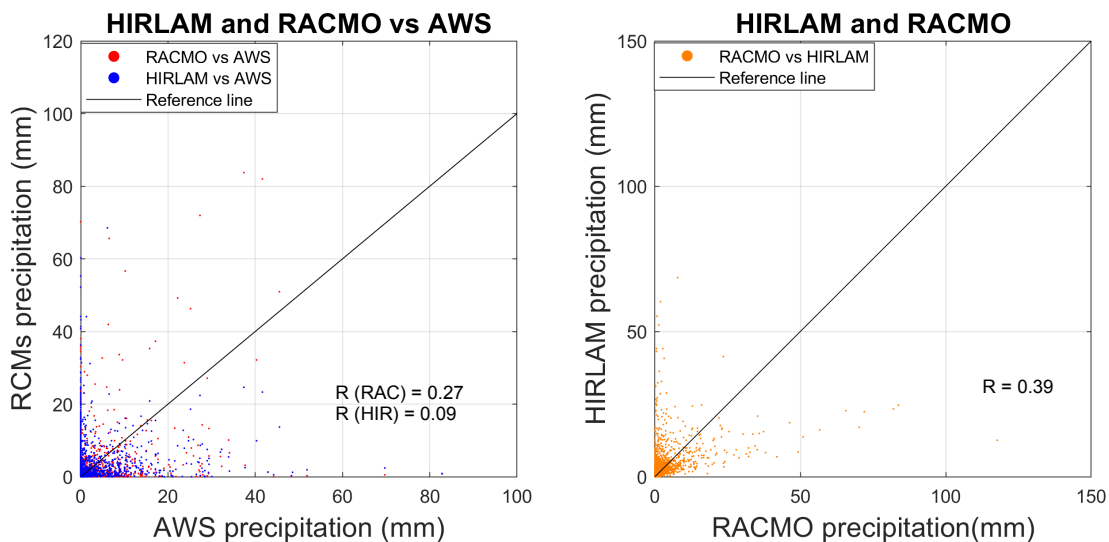

Figure 12. Scatterplot of RCMs vs AWS (left) and scatterplot of HIRLAM vs RACMO (right).

Precipitation for the AWS was calculated by using the measured snow depth and the snow density was assumed to be the same over the entire time span. This makes it a rather rough estimate and could thereby affect the accuracy of the calculated

precipitation. However, the assumed snow density is still deemed fairly representative of the conditions on Nordenskiöldbreen, where windy conditions lead to rapid compaction of snow. Since the location and altitude of the AWS and models differ, they receive different amounts of precipitation. Precipitation often occur during storms, during which the wind speed is high, causing snow to drift and the AWS to record lower values than the models. Across a surface as large as Nordenskiöldbreen there are local variations in precipitation, which could contribute to the differences between the RCMs and AWS (Van Pelt et al. 2014). The AWS only records snow depth for one specific point, whereas the two RCMs cover greater areas. If the station is not located at a representative point for this parameter, it might therefore cause a difference in values. Overall, RACMO performs better than HIRLAM for this parameter, possibly due to its smaller cell size. The bias is lower and the correlation coefficient is higher between RACMO and the AWS.

Using snow depth to estimate precipitation comes with a lot of uncertainties and the models might be better suited for determining precipitation than the AWS is. Other approaches such as using snow pillows, which measure the water equivalent directly, could provide different values. Snow pillows are however more difficult to maintain and might therefore not provide accurate measurements at a location such as Nordenskiöldbreen.

3.5. Cloud cover

In the plots of cloud cover over time, the different climate models and the AWS agree to some extent (Figure 13). In monthly time resolution, certain trends can be observed to be followed by both the RCMs and the AWS. When looking at the daily and 3 hourly resolution plots, there are very rapid changes in cloud cover and the different data sources provide rather different values. According to the correlation coefficients in Figure 14, the two RCMs have a moderate level of positive correlation with the AWS, both with values close to 0.53. When the models are compared with each other, they return a higher correlation coefficient of 0.63. The bias was lower for RACMO-AWS than for HIRLAM-AWS, 0.61% vs 8.73%. The RMS was large for all data sources, between 36.39% and 38.89%. HIRLAM has the highest mean, 65.67%, while RACMO and the AWS have values of 57.57% and 56.96% respectively.
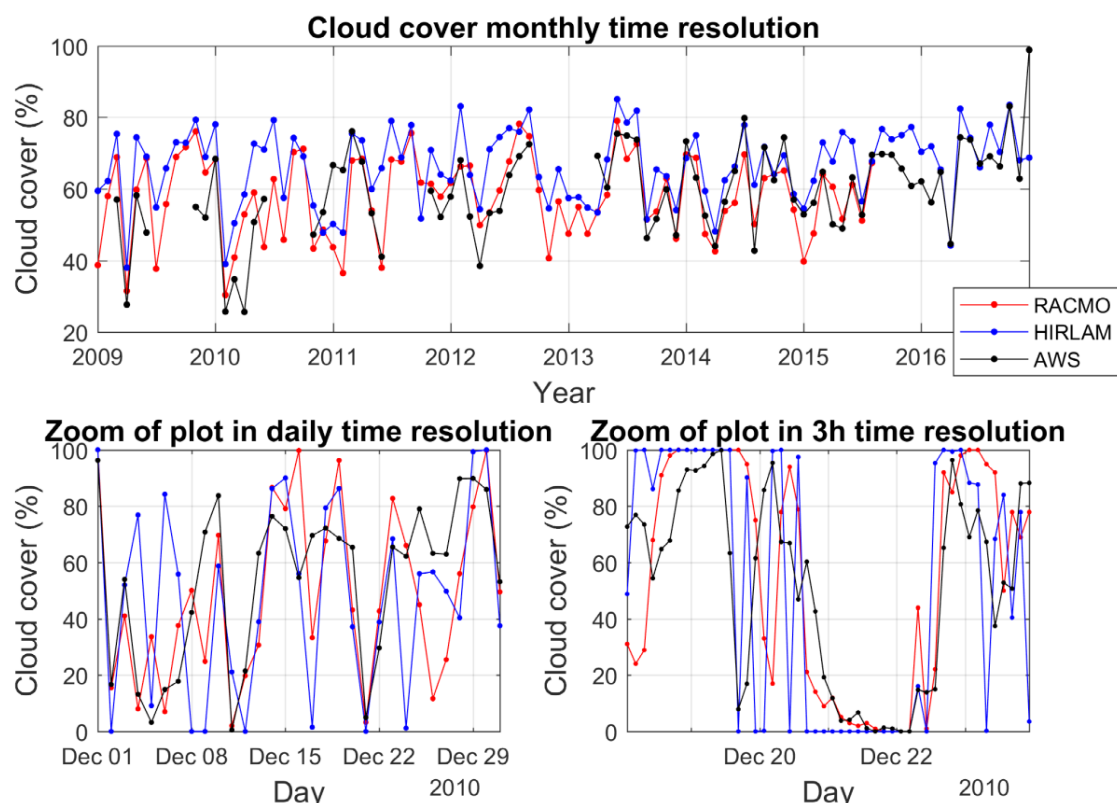
Figure 13. Plots of cloud cover vs time in monthly (top), daily (bottom left) and 3 hour (bottom right) time resolutions.
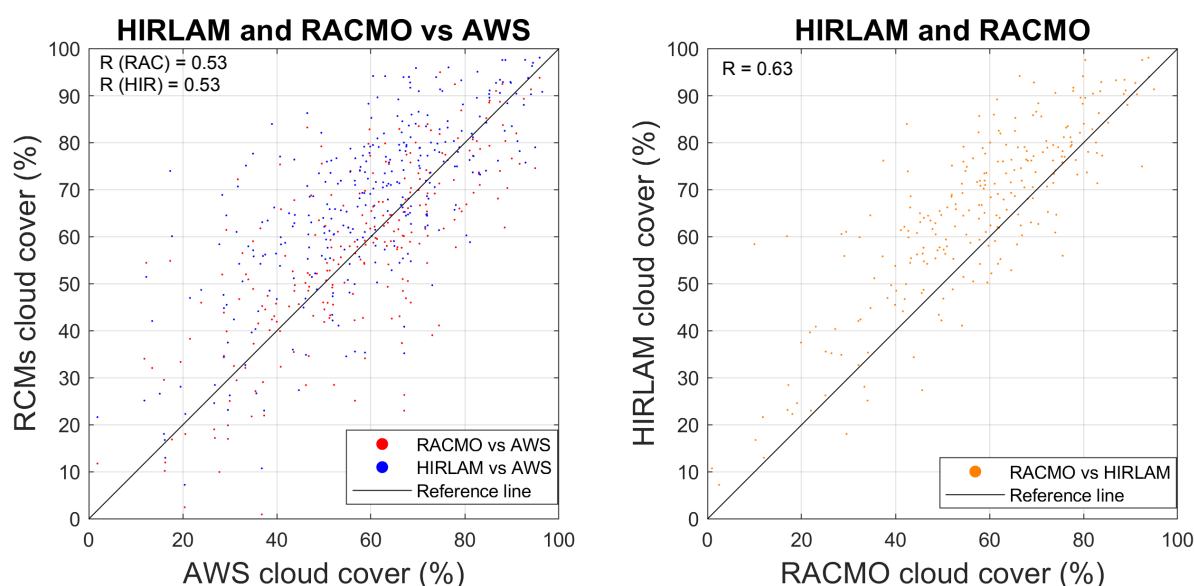

Figure 14. Scatterplot of RCMs vs AWS (left) and scatterplot of HIRLAM vs RACMO (right) in weekly time resolution.

Since the station does not measure cloud cover, it had to be calculated, therefore the data used for the comparison is an indirect estimate rather than a direct observation. Comparisons against the models were made nonetheless. Since the correlation coefficient between the models is higher than the ones against the station, it means that the models give values that are closer to each other than to the station. Either both of them might miscalculate in the same way, or perhaps more likely, the calculation of the station's cloud cover is inexact. Since the estimation of cloud cover

15

was based on assuming that the 10% highest values in a 1° temperature span represented 100% cloud cover, the resulting values might wrong if the percentage is off.

The bias was lower between RACMO and the AWS than between HIRLAM and the AWS, which suggests that HIRLAM overestimates the cloud cover. Because the RMS was large for all data sources, all datasets are likely to contain substantial errors. HIRLAM has the highest mean, which together with the bias and the RMS suggests that RACMO might be better at estimating cloud cover, assuming that the calculated cloud cover of the station is correct.

3.6. Wind

Wind speed over Nordenskiöldbreen follow similar trends for both RACMO and the AWS (Figure 15). In 3 hour time resolution, it appears that RACMO reports more even wind speeds, while the AWS measures more drastic changes.
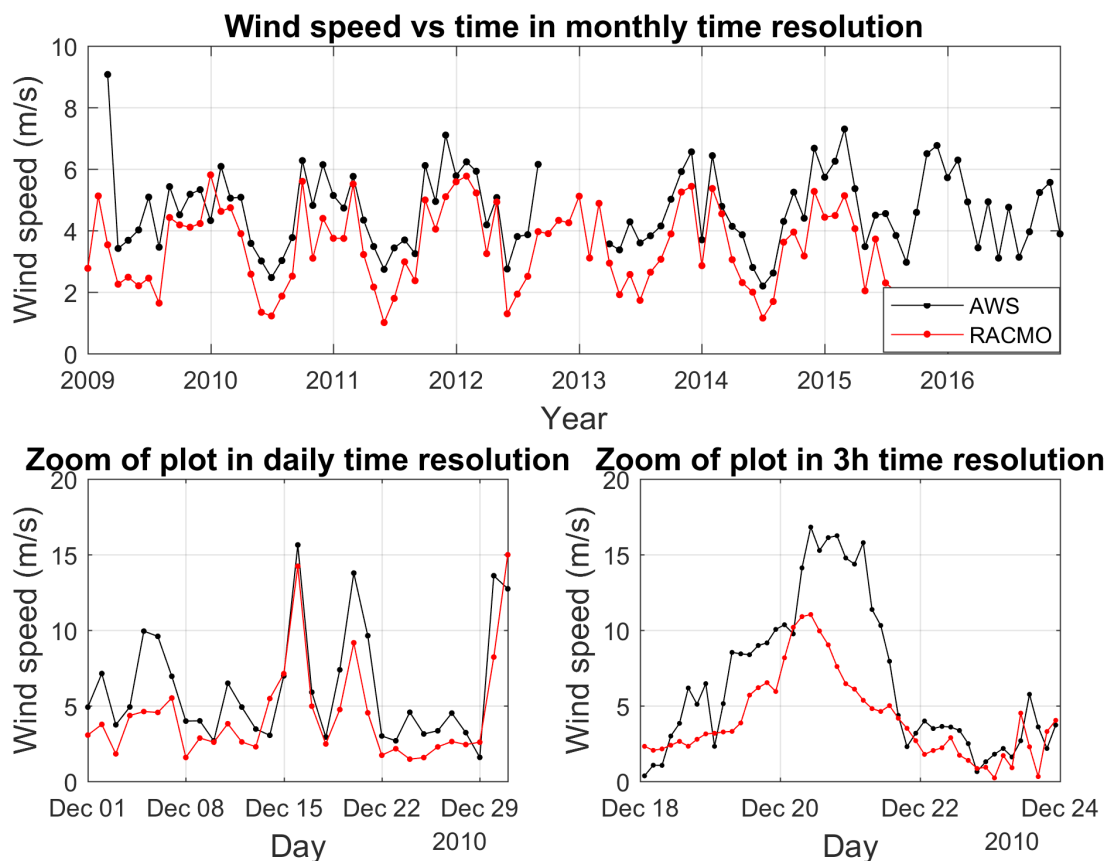

Figure 15. Wind speed vs time in different time resolutions. RACMO data ended on 31/8 2015.

The wind measured by the AWS is reported mainly from 30/35° N/NE. RACMO measures the main wind direction to be 60° N (Figure 16, Figure 17). The weather station records a larger spread in wind direction, whereas with RACMO the majority of wind seems to arrive from the same direction. Both sources report winds from 240° W/SW. The AWS measures wind from 330° NW that does not appear in the RACMO data. The mean wind speed for RACMO is 3.48 m/s and for the AWS it is 4.57 m/s. The RMS value of 2.76 m/s and the bias of -1.18 m/s
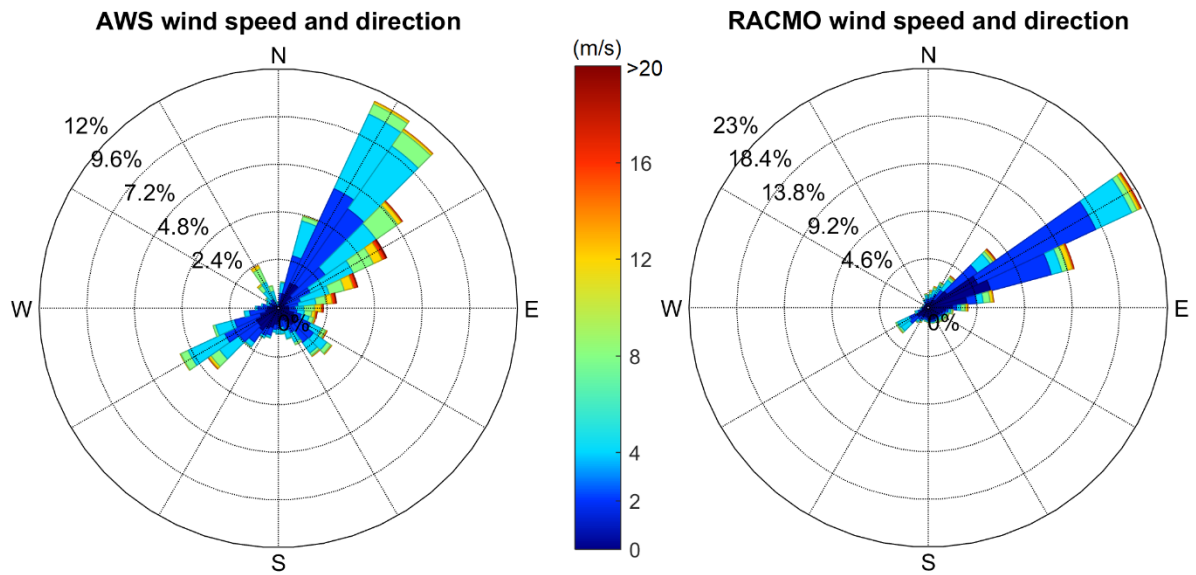
16

Figure 16. Wind rose diagram illustrating wind speed, direction and frequency over Nordenskiöldbreen as observed by the AWS (left) and simulated by RACMO (right).
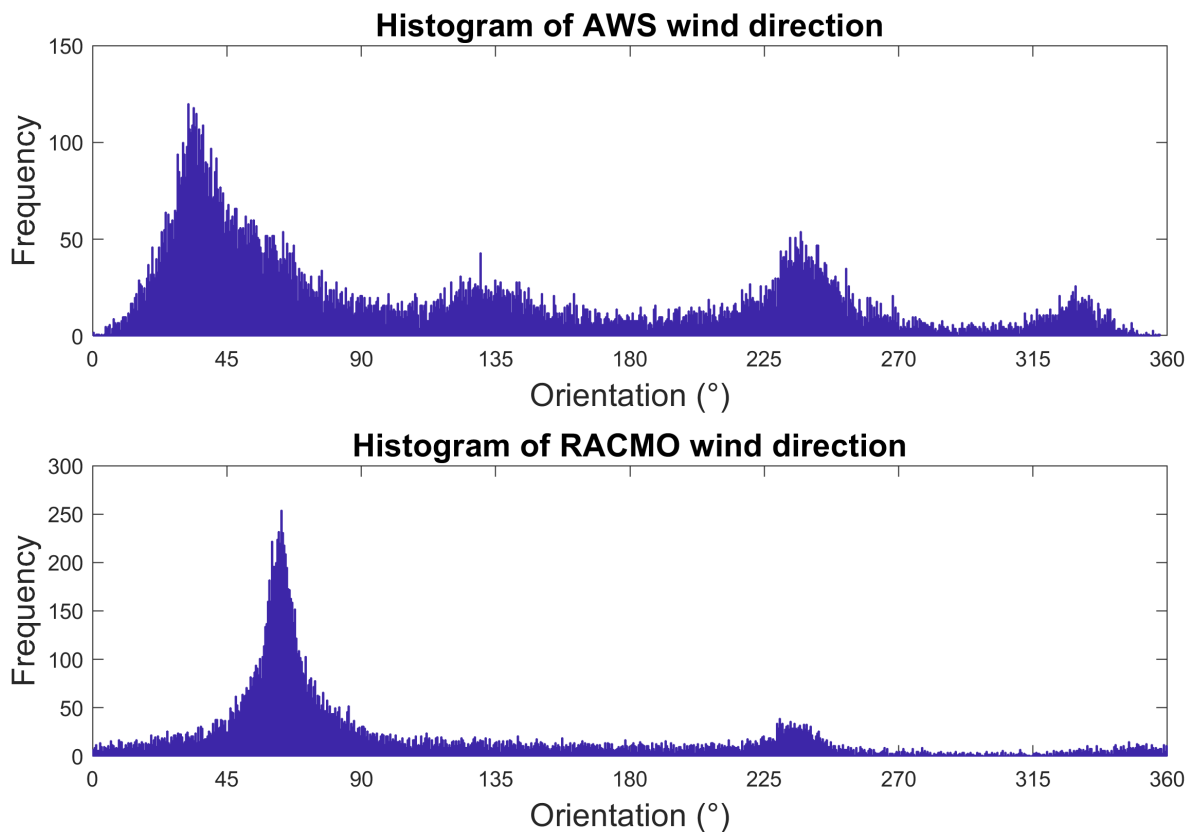

Figure 17. Histograms showing the frequency of wind directions as observed by the AWS (top) and simulated by RACMO (bottom).

RACMO estimates seasonal changes in wind speed well, following the same trend reported by the AWS with stronger wind in the winter half of the year and calmer periods in summer. Slow wind speeds are commonplace on glaciers such as Nordenskiöldbreen, but it appears RACMO continuously underestimates the strength

of the wind. The RMS and the bias further indicates RACMOs deviation from the in situ measurements.

The automatic weather station reports the main wind direction as being from 35° N/NE, with a lower frequency of winds from a variety of other directions. The latter is something RACMO does not include in its simulation, as it presents the wind arriving from 60° NE almost exclusively. Since most of incoming wind arrives from N/NE, the wind direction overlaps with the downslope direction of the glacier, which in combination with the slow wind speeds is indicative of katabatic wind. The occurrence of katabatic wind on Nordenskiöldbreen has been recorded by Claremar et al. (2012) and strengthens the credibility of the wind observed and simulated in this project. Both the AWS and RACMO report winds from 240° W/SW, the upslope direction of Nordenskiöldbreen, which could be the anabatic wind. The AWS records wind from 330° NW, which is not apparent in the RACMO data. As seen in the modelled elevation map (Figure 3), there are depressions in De Geerfjellet, which could potentially be the source where these winds pass through to the AWS. The reason RACMO does not report this could be due to the passage being too small for RACMO to register.

Although RACMO neglects certain factors in the terrain and underestimates the average wind speed, the general qualities of the wind are represented and could be used to give an overview of the conditions on Nordenskiöldbreen.

3.7.   Storm event

Figure 18 and Figure 19 shows the changes in the different parameters between the 6th and 11th of March 2010. Throughout the period, the temperature and the wind speed increase and reaches their peak on the 9th, before decreasing. During the same period, the air pressure does the opposite, which, in combination with the wind and temperature changes, indicates a storm event. The cloud cover shows overcast conditions during most of the event, which further strengthens the theory that a storm took place.

Snowfall and high wind speeds often coincide during storms, which agrees with the results from HIRLAM and the AWS. HIRLAM shows an increased precipitation, while the AWS, which is based on the snow depth, does not record any changes. This is because the weather station records snow depth, and therefore does not register the snowfall correctly due to the wind drift. Although, since RACMO does not capture any precipitation either, it is safest to disregard this parameter for this specific event. For the relative humidity, the models do not seem to agree with the AWS, which is not surprising considering the low correlations during the full time-series.

Generally, with exceptions for some parameters, the models capture the storm event well. This means that the RCMs could be useful for identifying such extreme events.
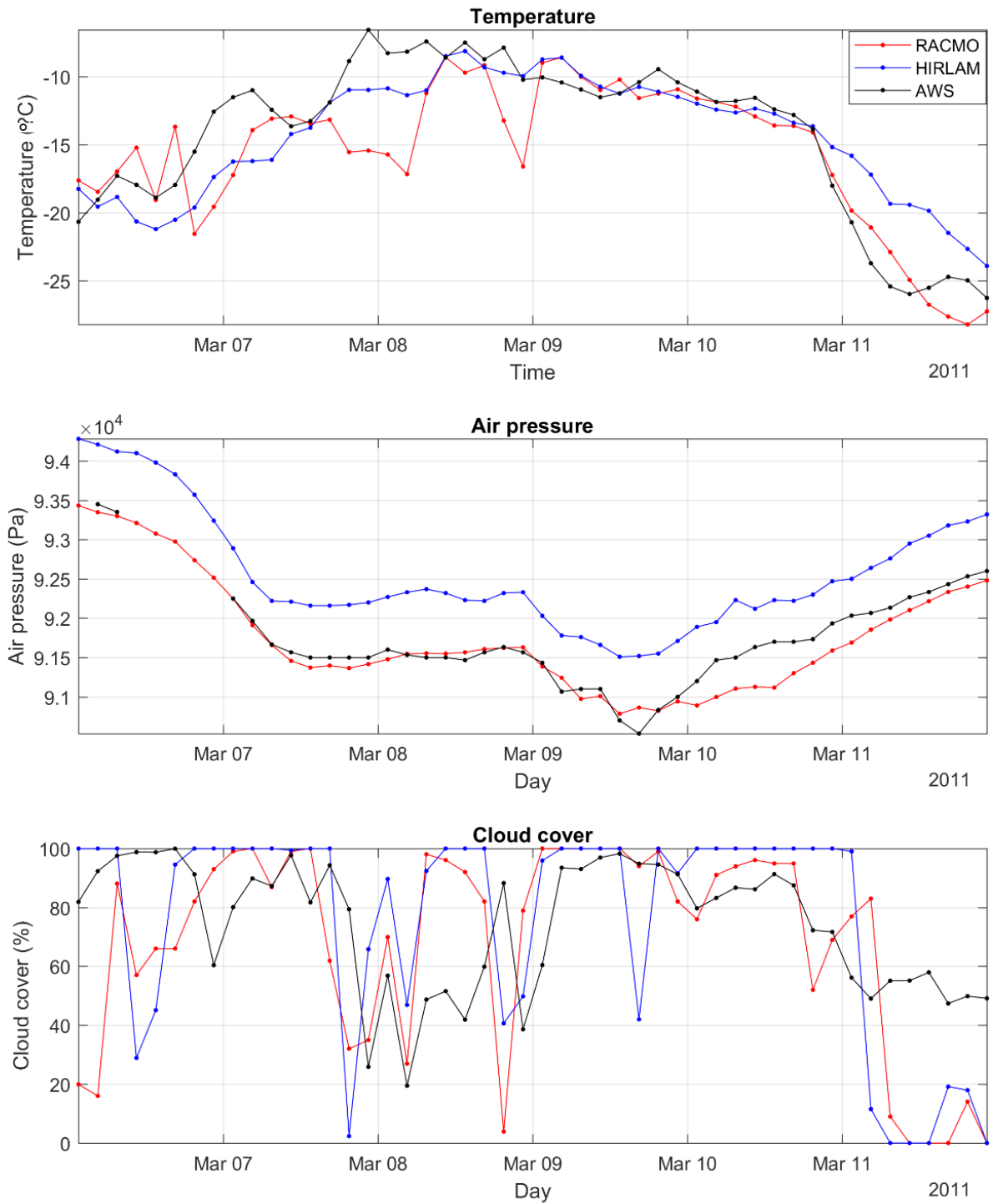
Figure 18. The changes in temperature (top), air pressure (middle) and cloud cover (bottom) between the 6th and 11th of March 2010.
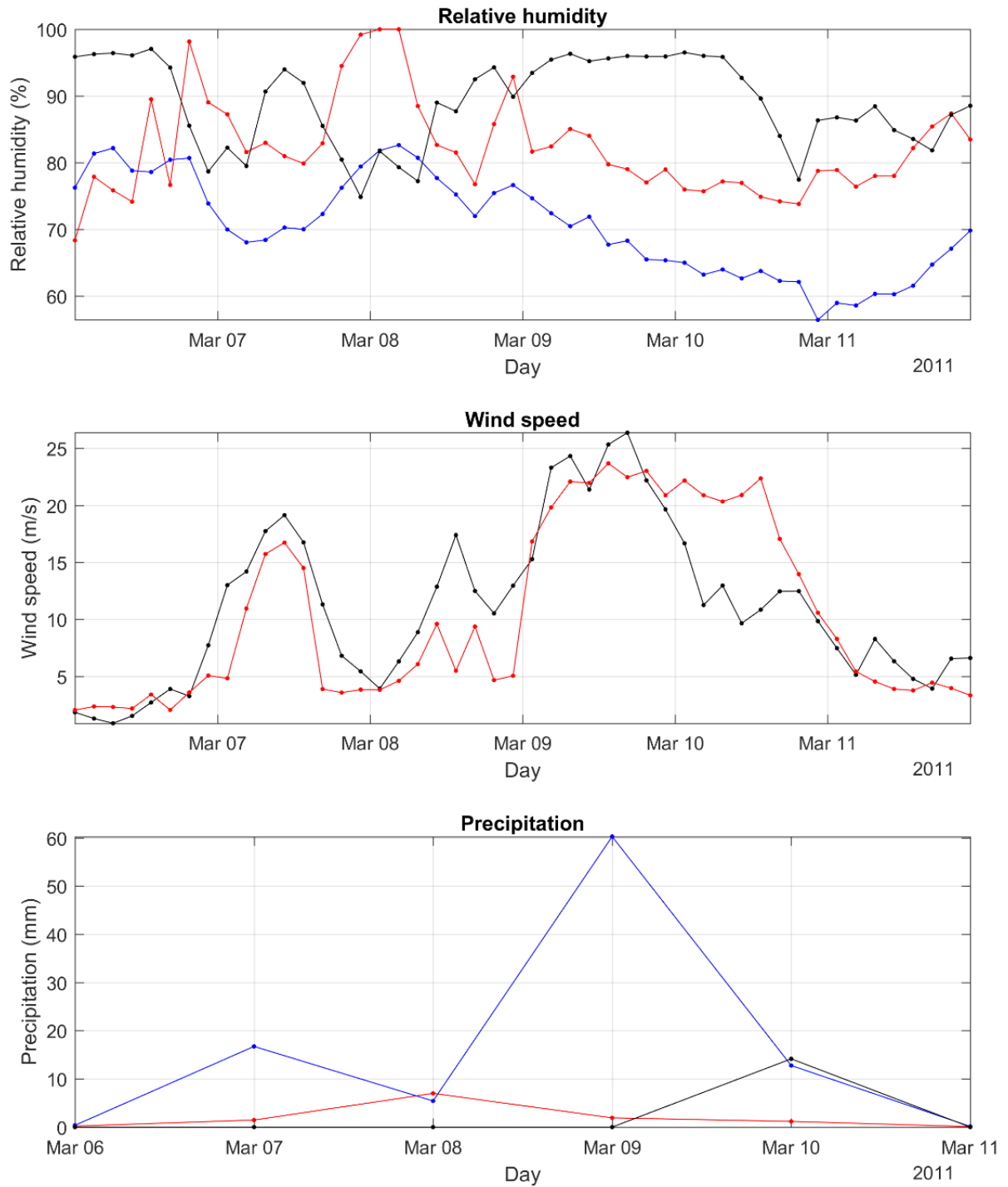
Figure 19. The changes in relative humidity (top), wind speed (middle) and precipitation (bottom) between the 6th and 11th of March 2010.

4.   Conclusion

In this project, we analysed the relationships between data from HIRLAM, RACMO and an automatic weather station located on Svalbard. Weather stations demand maintenance and only show measurements for a single location, limiting their coverage. RCMs have the advantage of more spatially distributed data and longer time-series compared to an AWS, in and are therefore more suitable as a forcing for distributed glacier mass balance modelling. For some of the parameters, the climate models return values with high similarity to the measurements taken in situ by the AWS. Temperature and air pressure are very well estimated by both models, and they can therefore be good alternatives to the AWS. Additionally, RACMO represents the wind speed and direction well. Poorer correlation is found for cloud cover, relative humidity and particularly precipitation.

RACMO and HIRLAM perform similarly well for most parameters, making it difficult to determine if one is more suited for modelling High Arctic climate than the other. In general, both HIRLAM and RACMO perform well and the meteorological data that they provide could be used for mass balance modelling. To ensure that the models' ability to simulate meteorological conditions is not limited to this particular area, comparisons with other weather stations can be done.

Acknowledgements

We want to thank our supervisor Ward van Pelt for guiding us through the creation of this project and helping us with all our questions.

References

Benn, D. I. & Evans, D. J. A. (1998). *Glaciers and Glaciation*. London. Arnold.

Bintanja, R. & van der Linden, E. C. (2013). The changing seasonal climate in the Arctic. *Scientific Reports,* 3, 1556.

Claremar, B., Obleitner, F., Reijmer, C., Pohjola, V., Waxegård, A., Karner, F. Rutgersson, A. (2012). Applying a Mesoscale Atmospheric Model to Svalbard Glaciers. *Advances in Meteorology*, 2012, Article ID 321649, 22 pages. DOI:10.1155/2012/321649.

Cogley, J. G., Hock, R., Rasmussen, L. A., Arendt, A. A., Bauder, A., Braithwaite, R.J., Jansson, P., Kaser, G., Möller, M., Nicholson, L., and Zemp, M. (2011) *Glossary of Glacier Mass Balance and Related Terms.* IHP-VII Technical Documents in Hydrology No. 86, IACS Contribution No. 2, UNESCO-IHP. Paris.

Den Ouden, M. A. G., Reijmer, C. H., Pohjola, V., Van de Wal, R. S. W., Oerlemans, J., and Boot, W. (2010). Stand-alone single-frequency GPS ice velocity observations on Nordenskiöldbreen, Svalbard, *The Cryosphere*, 4(4), pp 593-604, DOI:10.5194/tc-4-593-2010.

Ebrahimi, S. & Marshall, S. J. (2016). Surface energy balance sensitivity to meteorological variability on Haig Glacier, Canadian Rocky Mountains. *The Cryosphere,* 10(6), pp 2799–2819.

Hagen, J. O., Kohler J., Melvold, K. & Winther, J. (2003). Glaciers in Svalbard: mass balance, runoff and freshwater flux. *Polar Research*, 22(2), pp 145–159.

IPCC. (2013): *Climate Change 2013: The Physical Science Basis*. Contribution of Working Group I to the Fifth Assessment Report of the Intergovernmental Panel on Climate Change [Stocker, T. F., D. Qin, G.-K. Plattner, M. Tignor, S. K. Allen, J. Boschung, A. Nauels, Y. Xia, V. Bex and Midgley, P. M. (eds.)] Cambridge University Press, Cambridge, United Kingdom and New York, NY,   USA

Kuipers Munneke P., Reijmer C. H. & van den Broeke M. R. (2011). Assessing the retrieval of cloud properties from radiation measurements over snow and ice. *International Journal of Climatology,* 31(5), pp 756–769.

Noël, B., van de Berg, W. J., Machguth, H., Lhermitte, S., Howat, I., Fettweis, X. & van den Broeke, M. R. (2016). A daily, 1 km resolution data set of downscaled Greenland ice sheet surface mass balance (1958–2015). *The Cryosphere*, 10(5), pp 2361–2377.

Oerlemans, J. (2010). *The Microclimate of Valley Glaciers*. Utrecht, Utrecht University. Igitur, Utrecht Publishing & Archiving Services.

Reistad, M., Breivik, Ø., Haakenstad, H., Aarnes, O. J., Furevik, B. R. & Bidlot, J. (2011). A high resolution hindcast of wind and waves for the North Sea, the Norwegian Sea, and the Barents Sea. *Journal of Geophysical Research: Oceans*, 116(C5).

Screen, J. & Simmonds, I. (2010). The Central Role of Diminishing Sea Ice in Recent Arctic Temperature Amplification. *Nature*, 464, pp 1334–7.

Serreze, M. C., Barrett, A. P., Stroeve, J. C., Kindig, D. N. & Holland, M. M. (2009). The emergence of surface-based Arctic amplification. *The Cryosphere*, 3(1), pp 11–19.

Tarbuck, E. J., Lutgens, F. K. & Tasa, D. G. (2014). *Earth: An Introduction to Physical Geology*. 11th ed. Harlow: Pearson.

Van Pelt, W. J. J. (2014) *Modelling the dynamics and boundary processes of Svalbard glaciers*. Diss. Utrecht, Netherlands: University of Utrecht.

Van Pelt, W. J. J. and Kohler, J. (2015). Modelling the long-term mass balance and firn evolution of glaciers around Kongsfjorden, Svalbard. *Journal of Glaciology*, 61(228), pp 731-744. DOI:10.3189/2015JoG14J223

Van Pelt, W. J. J., Oerlemans, J., Reijmer, C. H., Pohjola, V. A., Pettersson, R. and Van Angelen, J. H. (2012). Simulating melt, runoff and refreezing on Nordenskiöldbreen, Svalbard, using a coupled snow and energy balance model. *The Cryosphere*, 6(3), pp 641-659. DOI:10.5194/tc-6-641-2012

Van Pelt, W. J. J., Pettersson, R., Pohjola, V. A., Marchenko, S., Claremar, B., and Oerlemans, J. (2014). Inverse estimation of snow accumulation along a snow radar transect on Nordenskiöldbreen, Svalbard. *Journal of Geophysical Research: Earth Surface*, 119(4), pp 816-835. DOI:10.1002/2013JF003040

Van Pelt W.J.J., V.A. Pohjola., R. Pettersson., L.E. Ehwald., C. Reijmer., W. Boot., & S. Jakobs. (2018). Dynamic response of a High Arctic glacier to melt and runoff variations. Geophysical Research Letters, 45. DOI: 10.1029/2018GL077252.

Van Pelt, W. J. J., Pohjola, V. A. & Reijmer, C. H. (2016). The Changing Impact of Snow Conditions and Refreezing on the Mass Balance of an Idealized SvalbardGlacier. *Frontiers in Earth Science*, 4(102). DOI: 10.3389/feart.2016.00102

Vihma, T., Tuovinen, E., & Savijärvi, H. (2011). Interaction of katabatic winds and near-surface temperatures in the Antarctic. Journal of Geophysical Research, 116(D21). DOI: 10.1029/2010JD014917.

Walczowski, W., & Piechura, J. (2006). New evidence of warming propagating toward the Arctic Ocean. Geophysical Research Letters, 33(L12), L12,601. DOI: 10.1029/2006GL025872

Appendix

MATLAB functions used to calculate the results:

annotation
axis
box
colorbar
diff
discretize
double
hist
hold
interp1
isfinite
isnan
figure
findall
grid
legend
load
max
nanmean
pcolor
plot
refline
repelem
rms
round
scatter
set
shading
size
sortrows
subplot
sum
synchronize
table
timerange
timetable
title
unique
xlabel
xlim
ylabel